Research Article | Vol. 28, No. 21 / 12 October 2020 / Optics Express 30447
Optics EXPRESS

Aberration fields of pupil-offset off-axis two-mirror astronomical telescopes induced by ROC error

XIAOQUAN BAI,[1,2] BOQIAN XU,[1] HONGCAI MA,[1,3] YAN GAO,[1] SHUYAN XU,[1] AND GUOHAO JU[1,4]

[1]*Changchun Institute of Optics, Fine Mechanics and Physics, Chinese Academy of Sciences, Changchun, Jilin 130033, China*
[2]*University of Chinese Academy of Sciences, Beijing 100049, China*
[3]*mahc@ciomp.ac.cn*
[4]*juguohao@ciomp.ac.cn*

Abstract: This paper presents a systematic and deep discussion on the aberration field characteristics of pupil-offset off-axis two-mirror astronomical telescopes induced by the radius of curvature (ROC) error based on the framework of the nodal aberration theory (NAT). The expressions of the third-order aberrations in off-axis two-mirror astronomical telescopes with ROC error are derived first. Then the astigmatic and coma aberration fields are discussed, and it is shown in a field constant astigmatism and coma will be induced by ROC error. The aberration compensation between axial misalignments and ROC error are further discussed, and it is shown that the net astigmatic and coma aberration field induced by ROC error can well be compensated by axial misalignments. Importantly, it is also demonstrated that the focal plane shift induced by ROC error can also be compensated at the same time. Also, this paper briefly analyzes the aberration field characteristics when there is the error of conic constant in optical system. Some other discussions are also presented concerning the ROC inconsistency in astronomical telescopes with a segmented primary mirror. This work will lead to a deep understanding of the influence of ROC error in pupil-offset off-axis astronomical telescopes.

1. Introduction

Comparing with on-axis astronomical telescopes, there are a great number of advantages for pupil-offset off-axis ones in astronomical observation, such as scattering property, emissivity throughput and dynamic range [1,2]. The performance of pupil-offset off-axis telescopes relies on control of aberrations that arise from limitations in the alignment and manufacture. In recent years, Nodal aberration theory (NAT) [3–10] had been extended to pupil-offset off-axis telescopes and the aberration fields of different kinds of misalignments (lateral, axial and rotational misalignments) have been deeply investigated [11–13] (NAT has been an powerful analytic tool in discussing the characteristic aberration field dependencies induced by surface decenters/tip-tilts but it is only directly applicable to optical systems composed of individually rotationally symmetric surfaces). These researches can contribute to an in-depth understanding for the alignment of pupil-offset off-axis telescopes.

It is also of great significance to study the influence of ROC error on the net aberration fields. On one hand, ROC error is one of most common manufacture errors. This kind of error not only can influence the imaging quality of optical system, but also change the position of focal plane, which should be determined precisely. Therefore, ROC error has a great impact on the assembly, integration and test of large astronomical telescopes on the ground. On the other hand, for space telescopes, the variation in the temperature, gravity and the structure of support can also induce the ROC error. We also need to consider how to compensate the influence of ROC error on orbit.

#403470 https://doi.org/10.1364/OE.403470
Journal © 2020 Received 23 Jul 2020; revised 6 Sep 2020; accepted 16 Sep 2020; published 28 Sep 2020

Optics EXPRESS

Besides, in the process of optical design, an in-depth understanding of the influence of ROC error as well as the interactions between ROC error and misalignments of mirror can provide a theoretical guidance on the process of tolerance distribution.

However, the influence of ROC error in pupil-offset off-axis telescopes due to manufacture error has not been studied deeply. In1975, some researchers clarified the required accuracy in the ROC of a primary astronomical telescope mirror based on the characteristic of aberration field for the on-axis system [14]. Some other researchers discussed the effects of ROC error in segmented telescopes. Rakoczy estimated the influence of global radius of curvature (GROC) for Hobby-Eberly Telescope [15]. Cheng presented a new approach to generate compensators that controls the local ROC of each segment efficiently for the segmented system [16]. However, we still lack some intuitive understanding on the influences of ROC in pupil-offset off-axis astronomical telescopes.

In this paper, we will present an in-depth and systematic discussion on the net aberration fields of ROC error in pupil-offset off-axis astronomical telescopes, with a famous off-axis two-mirror astronomical telescopes, New Solar Telescope (NST), as an example. The main contents of this paper include analytically expressing of effects of the ROC error on the aberration fields, illuminating the aberration field characteristics induced by ROC error and discussing the aberration compensation between ROC error and axial misalignments. Meanwhile, the influences of conic error are also discussed. Besides, we discuss the inconsistency of ROC in segmented telescopes and point out it can no longer be compensated with axial misalignments.

This paper is organized as follows. In Section 2, we derive the aberration function of off-axis two-mirror astronomical telescopes in the presence of ROC error. In Section 3, astigmatic and coma aberration field characteristic induced by ROC error are discussed. Then the interactions between ROC error and axial misalignments are investigated in Section 4. The astigmatic and coma aberration fields induced by the conic error are further discussed. Some other discussions concerning the ROC error in segmented primary mirror (PM) are presented in Section 6. We summarize and conclude this paper in Section 7.

2. Aberration function of off-axis two-mirror astronomical telescopes in the presence of the error of the structure parameters

Based on the system-level pupil coordination transformation and third-order NAT, the aberration function of off-axis two-mirror astronomical telescopes with the error of the structure parameters will be derived. Then, the focus will be on specific expressions of astigmatism, coma and defocus, which are related to optical system parameters.

The wave aberration function of pupil-offset off-axis optical systems can be expressed as [17]

$$W_{off-axis} = \sum_{j} \sum_{p=0}^{\infty} \sum_{n=0}^{\infty} \sum_{m=0}^{\infty} (W_{klm}^{(sph,asph)})_j (\vec{H} \cdot \vec{H})^p \cdot [(\vec{\rho} + \vec{s}) \cdot (\vec{\rho} + \vec{s})]^n (\vec{H} \cdot \vec{\rho})^m, \quad k = 2p + m, l = 2m + n, \tag{1}$$

where $\overrightarrow{H}$ is the normalized field vector, $\vec{\rho}$ is the normalized pupil vector of off-axis telescope, $\vec{s}$ represents the location of the off-axis pupil relative to the on-axis pupil which is also normalized by semi-diameter of the off-axis aperture and $(W_{klm}^{(sph,asph)})_j$ denotes the aberration coefficient for a particular aberration type of spherical and aspheric surface j, meanwhile, W_{klmj} would be rewritten as $W_{klmj}^{(sph,asph)} = W_{klmj}^{sph} + W_{klmj}^{asph}$ in the following, where the super-script *sph* denotes that the aberration coefficient is for the base sphere and *asph* denotes that it is for the aspheric departure from the base sphere. In order to highlight characters of the aberration field, only

Optics EXPRESS

consider the third-order aberrations, Eq. (1) can be rewritten as

$$\begin{aligned} W_{off-axis}^{3rd}(\vec{H},\vec{\rho}) = {} & (W_{020}+\Delta W_{020})(\vec{\rho}+\vec{s})^2 \\ & + \sum_j (W_{040j}^{sph}+W_{040j}^{asph})[(\vec{\rho}+\vec{s})\cdot(\vec{\rho}+\vec{s})]^2 \\ & + \sum_j (W_{131j}^{sph}+W_{131j}^{asph})[\vec{H}\cdot(\vec{\rho}+\vec{s})][(\vec{\rho}+\vec{s})\cdot(\vec{\rho}+\vec{s})] \\ & + \sum_j (W_{220Mj}^{sph}+W_{220Mj}^{asph})(\vec{H}\cdot\vec{H})[(\vec{\rho}+\vec{s})\cdot(\vec{\rho}+\vec{s})] \\ & + \frac{1}{2}\sum_j (W_{222j}^{sph}+W_{222j}^{asph})[\vec{H}^2\cdot(\vec{\rho}+\vec{s})^2] \\ & + \sum_j (W_{311j}^{sph}+W_{311j}^{asph})(\vec{H}\cdot\vec{H})[\vec{H}\cdot(\vec{\rho}+\vec{s})], \end{aligned} \tag{2}$$

where $W_{220M} = W_{220} + \frac{1}{2}W_{222}$. W_{040j}^{sph} and W_{040j}^{asph} present wave aberration coefficients for spherical aberration, W_{131j}^{sph} and W_{131j}^{asph} present aberration coefficients for coma, W_{222j}^{sph} and W_{222j}^{asph} present aberration coefficients for astigmatism, W_{220Mj}^{sph} and W_{220Mj}^{asph} present aberration coefficients for the medial focal surface, Here the subscript M for W_{220} means that the astigmatic aberration is measured with reference to the medial focal surface. W_{020} is related to the back working distance of optical system. W_{311j}^{sph} and W_{311j}^{asph} present aberration coefficients for distortion.

ROC error can affects the aberration coefficients of the on-axis parent system, $W_{klm}^{(sph,asph)}$. For off-axis two-mirror astronomical telescopes, the field of view (FOV) is usually very small. Comparing with the change of $W_{040}^{(sph,asph)}$, the change of $W_{222}^{(sph,asph)}$, $W_{131}^{(sph,asph)}$ and $W_{220M}^{(sph,asph)}$ can be ignored when ROC error is in a certain range [12]. The relationship between structural parameters (including ROC) and aberration coefficients $W_{040}^{(sph,asph)}$ for two-mirror astronomical telescopes with the aperture stop located at the PM is presented as follows [18]:

$$W_{040}^{(sph,asph)} = \frac{D^4m^3}{512(f'_{SYS})^3} + \frac{k_{PM}D^4m^3}{512(f'_{SYS})^3} + \frac{D^4(m+1)^2(1-m)\gamma}{512(f'_{SYS})^3} + \frac{k_{SM}D^4(1-m)^3\gamma}{512(f'_{SYS})^3}, \tag{3}$$

where D represents the entrance pupil diameter of the telescope, k_{PM} is the conic constant of the PM, k_{SM} is the conic constant of the secondary mirror (SM). $\gamma = \frac{y_{SM}}{y_{PM}}$ is the axial obstruction ratio of the system, $m \equiv -\frac{f'_{SYS}}{f'_{PM}}$ is the SM magnification, y_{PM} and y_{SM} denote the marginal-ray height on PM and SM, respectively, $f'_{SYS} = \frac{f'_{PM}f'_{SM}}{f'_{PM}-f'_{SM}-d_1}$ corresponds to the system focal length, and f'_{PM} and f'_{SM} denote the focal length of PM and focal length of SM, respectively (d_1 represents the distance between PM and SM).

Optics EXPRESS

In this paper, we mainly consider astigmatism, coma and defocus aberration induced by ROC error, which can be expressed as

$$
\begin{aligned}
W_{off-axis} = & \left\{ \begin{array}{l} \frac{1}{2}\sum\limits_j (W^{sph}_{222j} + W^{asph}_{222j})\vec{H}^2 \\ +2\sum\limits_j [(W^{sph}_{040oj} + W^{asph}_{040oj}) + (\Delta W^{sph}_{040j} + \Delta W^{asph}_{040j})]\vec{s}^2 \\ +\sum\limits_j (W^{sph}_{131j} + W^{asph}_{131j})\vec{H}\vec{s} \end{array} \right\} \cdot \vec{\rho}^2 \cdots Astigmatism \\
& + \left\{ \begin{array}{l} \sum\limits_j (W^{sph}_{131j} + W^{asph}_{131j})\vec{H} \\ +4\sum\limits_j [(W^{sph}_{040oj} + W^{asph}_{040oj}) + (\Delta W^{sph}_{040j} + \Delta W^{asph}_{040j})]\vec{s} \end{array} \right\} \cdot \vec{\rho}(\vec{\rho}\cdot\vec{\rho}) \cdots Coma \\
& + \left\{ \begin{array}{l} W_{020} + \Delta W_{020} \\ +\sum\limits_j 4[(W^{sph}_{040oj} + W^{asph}_{040oj}) + (\Delta W^{sph}_{040j} + \Delta W^{asph}_{040j})](\vec{s}\cdot\vec{s}) \\ +W_{220M}(\vec{H}\cdot\vec{H}) \\ +2W_{131}(\vec{s}\cdot\vec{H}) \end{array} \right\} \cdot (\vec{\rho}\cdot\vec{\rho}) \cdots Defocus \\
& + else,
\end{aligned}
\tag{4}
$$

where $W^{sph}_{040j} + W^{asph}_{040j} = W^{sph}_{040oj} + W^{asph}_{040oj} + \Delta W^{sph}_{040j} + \Delta W^{asph}_{040j}$. W^{sph}_{klmoj} and W^{asph}_{klmoj} are in nominal state. ΔW^{sph}_{040j} and ΔW^{asph}_{040j} are induced by structural parameters errors (including ROC error).

3. Astigmatic and coma aberration field in pupil-offset off-axis two-mirror astronomical telescopes in the presence of ROC error

It is well known that ROC error mainly causes defocus aberration in on-axis two-mirror astronomical telescopes. However, this is not the case for pupil-offset off-axis telescopes. In this section, we will analytically express and illustrate the net coma and astigmatic aberration field caused by ROC error in off-axis two-mirror astronomical telescopes.

3.1. Astigmatic and coma aberration field characteristics in the presence of the ROC error in primary mirror

Base on Taylor expansion, Eq. (3) can be rewritten as

$$
W^{(sph,asph)}_{040} = \sum_j W^{(sph,asph)}_{040oj} + K_{040r_1}\Delta r_1 + K_{040r_2}\Delta r_2 + o(\Delta r_1) + o(\Delta r_2) \tag{5}
$$

where r_1 and r_2 denote the ROC of PM and the ROC of SM, respectively. K_{040r_1} is the sensitivity of $W^{(sph,asph)}_{040}$ to r_1 and K_{040r_2} is the sensitivity of $W^{(sph,asph)}_{040}$ to r_2. $o(r_1)$ and $o(r_2)$ denote the high order term about r_1 and the high order term about r_2, respectively, their effects can be ignored in the physical model, and $o(r_1)$ and $o(r_2)$ will be ignored in the following. According to Eq. (3),

Optics EXPRESS

K_{040r_1} and K_{040r_2} can be expressed as

$$\begin{cases} K_{040r_1} = -3\dfrac{\left(\frac{D^4\gamma d_1^3 k_{PM}}{8r_2^3} - \frac{D^4\gamma d_1^2}{4r_2^2} - \frac{D^4\gamma d_1}{8r_2} - \frac{D^4\gamma d_1^3 k_{SM}}{8r_2^3}\right)}{r_1^4} \\ \qquad - 2\dfrac{\left(\frac{3D^4\gamma d_1^2 k_{SM}}{16r_2^3} + \frac{3D^4\gamma d_1^2}{16r_2^3} + \frac{D^4\gamma d_1}{4r_2^2} + \frac{D^4\gamma}{16r_2}\right)}{r_1^3} \\ \qquad + \dfrac{\left(\frac{3D^4\gamma d_1}{32r_2^3} + \frac{D^4\gamma}{16r_2^2} + \frac{3D^4\gamma d_1 k_{SM}}{32r_2^3}\right)}{r_1^2} \\ K_{040r_2} = -3\dfrac{D^4\gamma}{64f_{PM}'^3}\left[\dfrac{k_{SM}(-d_1^3 + 3f_{PM}'d_1^2 - 3f_{PM}'^2 d_1 + f_{PM}'^3)}{r_2^4}\right] \\ \qquad - 3\dfrac{D^4\gamma}{64f_{PM}'^3}\left(\dfrac{-d_1^3 + 3f_{PM}'d_1^2 - 3f_{PM}'^2 d_1 + f_{PM}'^3}{r_2^4}\right) \\ \qquad + 2\dfrac{D^4\gamma}{64f_{PM}'^3}\dfrac{(2f_{PM}'d_1 - d_1^2 - f_{PM}'^2)}{r_2^3} + \dfrac{D^4\gamma}{64f_{PM}'^3}\dfrac{(d_1 - f_{PM}')}{r_2^2} \end{cases}. \tag{6}$$

According to Eq. (4), the expressions for astigmatic and coma aberration fields are expressed as followed:

$$\begin{cases} W_{ast} = \dfrac{1}{2}\sum_j (W_{222j}^{sph} + W_{222j}^{asph})\vec{H}^2 \\ \qquad + 2\sum_j [(W_{040oj}^{sph} + W_{040oj}^{asph}) + (\Delta W_{040j}^{sph} + \Delta W_{040j}^{asph})]\vec{s}^2 \\ \qquad + \sum_j (W_{131j}^{sph} + W_{131j}^{asph})\vec{H}\vec{s} \\ W_{coma} = \sum_j (W_{131j}^{sph} + W_{131j}^{asph})\vec{H} \\ \qquad + 4\sum_j [(W_{040oj}^{sph} + W_{040oj}^{asph}) + (\Delta W_{040j}^{sph} + \Delta W_{040j}^{asph})]\vec{s} \end{cases}. \tag{7}$$

Equation (7) includes those aberration components existing in the nominal state. Here we only consider those net aberration contributions of ROC error and neglect those components in the nominal system. In this case, Eq. (7) can be rewritten as

$$\begin{cases} \Delta W_{ast} = 2(K_{040r_1}\Delta r_1 + K_{040r_2}\Delta r_2)\vec{s}^2 \\ \Delta W_{coma} = 4(K_{040r_1}\Delta r_1 + K_{040r_2}\Delta r_2)\vec{s} \end{cases}. \tag{8}$$

In Eq. (8), the change of spherical aberration coefficients is expressed as a linear combination of the ROC errors in PM and SM. It is shown that a field-constant astigmatism and coma will be induced in the field of view in the presence of ROC error. Besides, the directions of these two kinds of field constant aberration induced by ROC error is related to the direction of pupil decenter.

NST will be used to demonstrate the aberration field characteristics presented by this paper. The specific optical prescription and layout of this telescope are presented in the Appendix A. The Fringe Zernike coefficients for astigmatism (Z5/Z6) and coma (Z7/Z8) at special field points

Optics EXPRESS

would be used to verify the reliability of the model from the optical simulation software (CODE V or ZEMAX). Furthermore, the full field displays (FFDs) for astigmatism and coma over a ±0.03° field of view from the optical simulation software (CODE V) would be used to demonstrate the aberration field dependences expressed in Eq. (8).

Here we suppose the ROC error in the PM of NST is −0.2 mm and the ROC error in the SM of NST is −0.05 mm. The net astigmatism and coma are shown in Table 1, where column A represents the results obtained from optical simulation software for on-axis parent system, column B represent the results calculated with Eq. (8) for NST and column C represents the results obtained from optical simulation software for NST. Furthermore, the full field displays (FFDs) for astigmatism and coma over a ±0.03° field of view are shown in Fig. 1. Table 1 shows that the astigmatism and coma in NST is far more sensitive to ROC error than in its parent on-axis

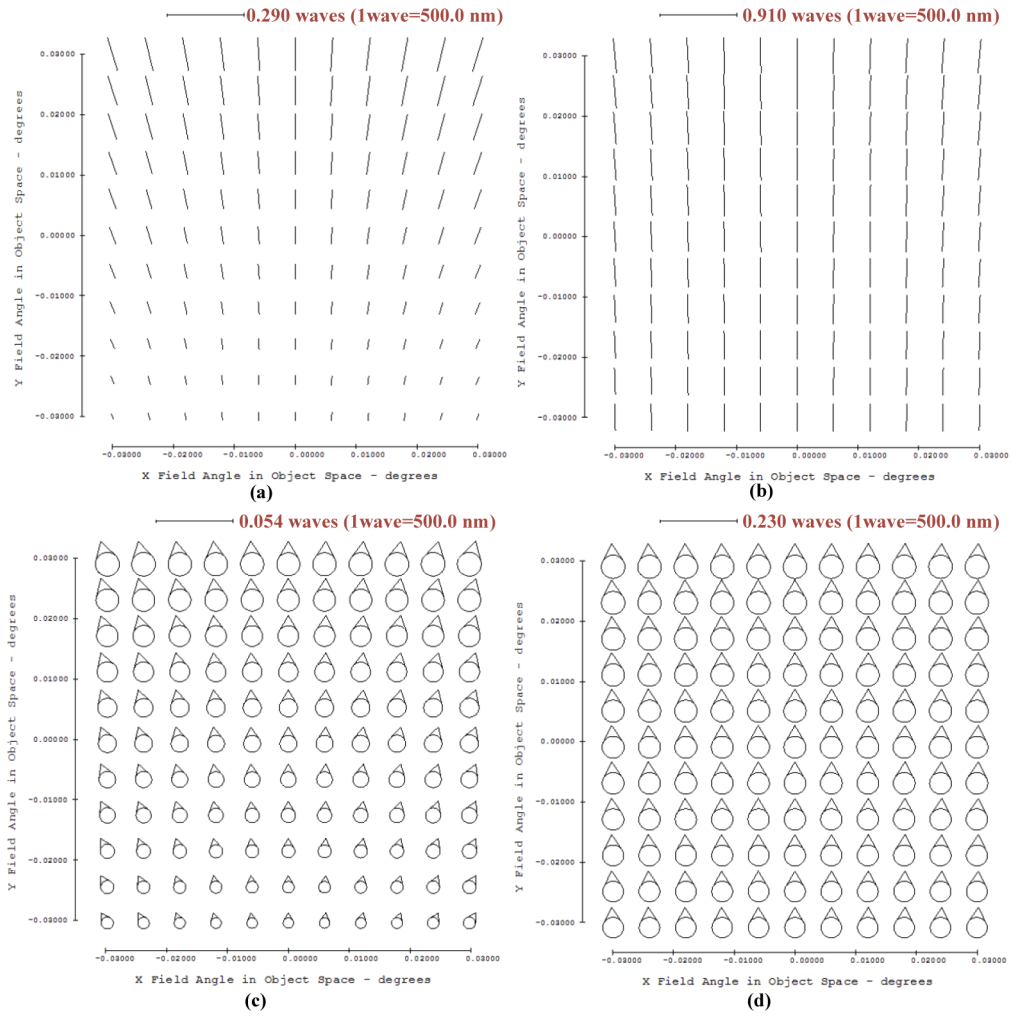

Fig. 1. FFDs for astigmatism (Z5/Z6) in the NST in nominal state (a) and in the presence of ROC errors of PM and SM (b). FFDs for coma (Z7/Z8) in the NST in nominal state (c) and in the presence of ROC errors of PM and SM (d). (b) and (d) show that in the presence of ROC errors of PM and SM, a large field-constant astigmatism and coma exists in the field of view.

Optics EXPRESS

system (especially astigmatism). Figure 1 demonstrates that a field-constant astigmatism and coma are induced in the effective field of view, which is consistent with the Eq. (8).

Table 1. Verification for the Expressions Describing the Astigmatic Aberration Field and the Coma Aberration Field when there are $\Delta r_1 = -0.2$mm and $\Delta r_2 = -0.05$mm in NST and its Parent System

		A	B	C
$(0°, 0°)$	ΔC_5	0.00	−0.36	−0.30
	ΔC_6	0.00	0.00	0.00
	ΔC_7	0.00	0.00	0.00
	ΔC_8	0.00	0.11	0.08
$(0°, 0.03°)$	ΔC_5	0.00	−0.36	−0.30
	ΔC_6	0.00	0.00	0.00
	ΔC_7	0.00	0.00	0.00
	ΔC_8	0.00	0.11	0.08

4. Aberration interactions between axial misalignments and ROC error

This section discusses compensating the effects of ROC error using axial misalignments. It is shown that the field-constant astigmatism and coma induced by ROC error can be well compensated with axial misalignments of the SM. Importantly, we demonstrate that the focal plane is nearly unchanged after aberration compensation compared to the nominal state.

4.1. Astigmatic aberration field and coma aberration field in the process of compensation

Referring to Eq. (7) and Eq. (8) from [19], we can get

$$W_{040}^{(sph,asph)} = \sum_j W_{040oj}^{(sph,asph)} + K_{040d_1}\Delta d_1 + o(d_1), \tag{9}$$

where k_{040d_1} is the sensitivity of $W_{040}^{(sph,asph)}$ to d_1, which can be expressed as

$$\begin{aligned} K_{040d_1} = &\frac{D^4\gamma}{512}\cdot\frac{-3d_1^3 + 2(3f'_{PM} - 4f'_{SM})d + (8f'_{PM}f'_{SM} - 4f'^2_{SM} - 3f'^2_{PM})}{f'^3_{PM}f'^3_{SM}} \\ &+ \frac{D^4\gamma}{512}\cdot k_{SM}\cdot\frac{-3d_1^2 + 6f'_{PM}d_1 - 3f'^2_{PM}}{f'^3_{PM}f'^3_{SM}}. \end{aligned} \tag{10}$$

Referring to Eq. (4), it is shown that both of the misalignments and ROC error of PM can affect $W_{040}^{(sph,asph)}$. Therefore, this property can be used to reduce the effects of ROC error using axial misalignments.

The condition for aberration compensation is $\Delta W_{040r_1}^{(sph,asph)} + \Delta W_{040d_1}^{(sph,asph)} = 0$, which can be rewritten as

$$K_{040d_1}\Delta d_1 = -K_{040r_1}\Delta r_1. \tag{11}$$

Here we only consider the effects of ROC error in the PM, considering that the ROC error in the SM is usually very small compared to PM. Therefore, we neglect the effects of ROC error in the SM for simplicity. Then the axial misalignment of SM needed for compensating the effects of

Optics EXPRESS

ROC error of the PM can be expressed as

$$\Delta d_1 = -\frac{K_{040r_1}\Delta r_1}{K_{040d_1}} \approx \frac{1}{2}\Delta r_1. \tag{12}$$

The derivation of the Eq. (12) is presented in the Appendix B, and we can refer to Fig. 2 to know the meaning of each structure parameter. Importantly, we can see from Eq. (12) that the axial misalignment of SM used to compensate for the effects of ROC error of PM is about half the ROC error.

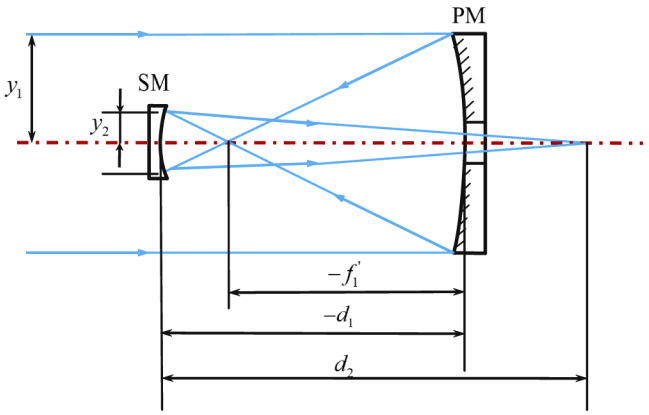

Fig. 2. The Gaussian optics of a two-mirror telescope

The NST is used as an example to verify the reliability of Eq. (12), as shown in Fig. 3, where the random ROC error of PM is $\Delta r_1 = -0.2$mm. Then Eq. (12) is used to calculate the compensating distance ($\Delta d_1 = -0.1$mm). Figure 3 demonstrates that the FFDs for astigmatism and coma after compensation is close to the ones in the nominal state. The actual distribution is consistent with the theory. In effect, we find that even an extremely large of ROC error (tens of millimeter) can also be compensated by changing the axial distance between PM and SM according to Eq. (12).

4.2. Defocus aberration in the process of aberration compensation

According to Eq. (4) that defocus aberration can be expressed as

$$W_{defocus} = \left\{ \begin{array}{l} \sum\limits_j 4[(W_{040oj}^{sph} + W_{040oj}^{asph}) + (\Delta W_{040j}^{sph} + \Delta W_{040j}^{asph})](\vec{s}\cdot\vec{s}) \\ (W_{020} + \Delta W_{020}) + W_{220M}(\vec{H}\cdot\vec{H}) + 2W_{131}(\vec{s}\cdot\vec{H}) \end{array} \right\} \cdot (\vec{\rho}\cdot\vec{\rho}). \tag{13}$$

The net defocus aberration induced by ROC error and axial misalignments can be written as

$$\Delta W_{defocus} = [\Delta W_{020} + (\Delta W_{040j}^{sph} + \Delta W_{040j}^{asph})(\vec{s}\cdot\vec{s})] \cdot (\vec{\rho}\cdot\vec{\rho}). \tag{14}$$

The relationship between ΔW_{020} and structure parameters is first established. The distance between Gaussian image plane and SM can be calculated by

$$l_{F'} = f'_{SYS}\left(1 - \frac{2d_1}{r_1}\right), \tag{15}$$

Considering $f'_{SYS} = \frac{r_1 r_2}{2r_1 - 2r_2 - 4d_1}$, Eq. (15) can be rewritten as

$$l_{F'} = \frac{r_1 r_2}{2r_1 - 2r_2 - 4d_1}\left(1 - \frac{2d_1}{r_1}\right). \tag{16}$$

Optics EXPRESS

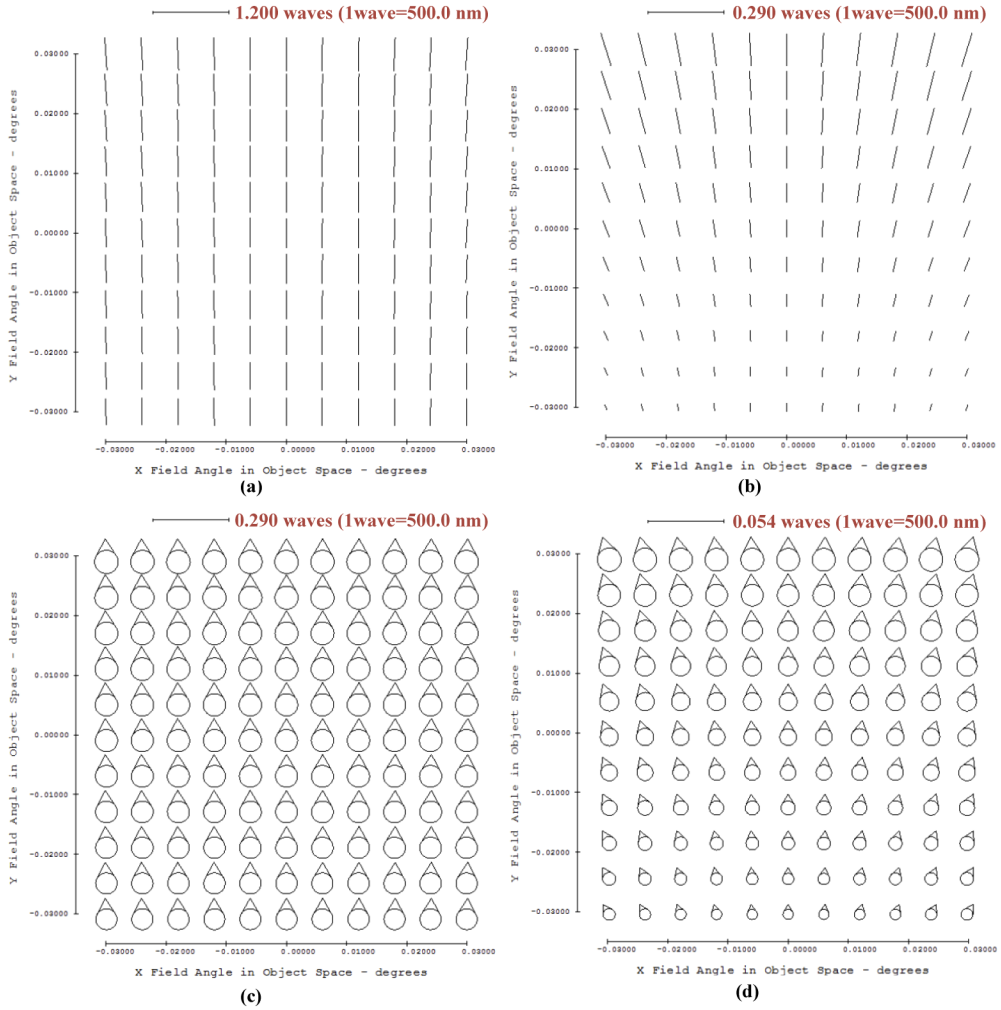

Fig. 3. FFDs for astigmatism (Z5/Z6) and coma (Z7/Z8) in the presence of (a, c) ROC error of PM and (b, d) after compensating the astigmatism induced by the ROC error of PM with axial misalignments. We can see that (b) and (d) are close to the nominal state comparing with Figs. 1(a) and (c).

Optics EXPRESS

The distance between PM and Gaussian image plane can be expressed as

$$l_{pF'} = \frac{r_1 r_2}{2r_1 - 2r_2 - 4d_1}\left(1 - \frac{2d_1}{r_1}\right) + d_1. \tag{17}$$

Then, we have

$$\Delta l_{pF'} = \frac{-2r_2^2}{(2r_1 - 2r_2 - 4d_1)^2}\Delta r_1. \tag{18}$$

According to $\Delta W_{020} = \frac{\Delta Z}{8(F^{\#})^2}$, where ΔZ presents the distance between actual image plane and Gaussian image plane, and $F^{\#} = \frac{f'_{SYS}}{D}$. The relationship between ΔW_{020} and structure parameters

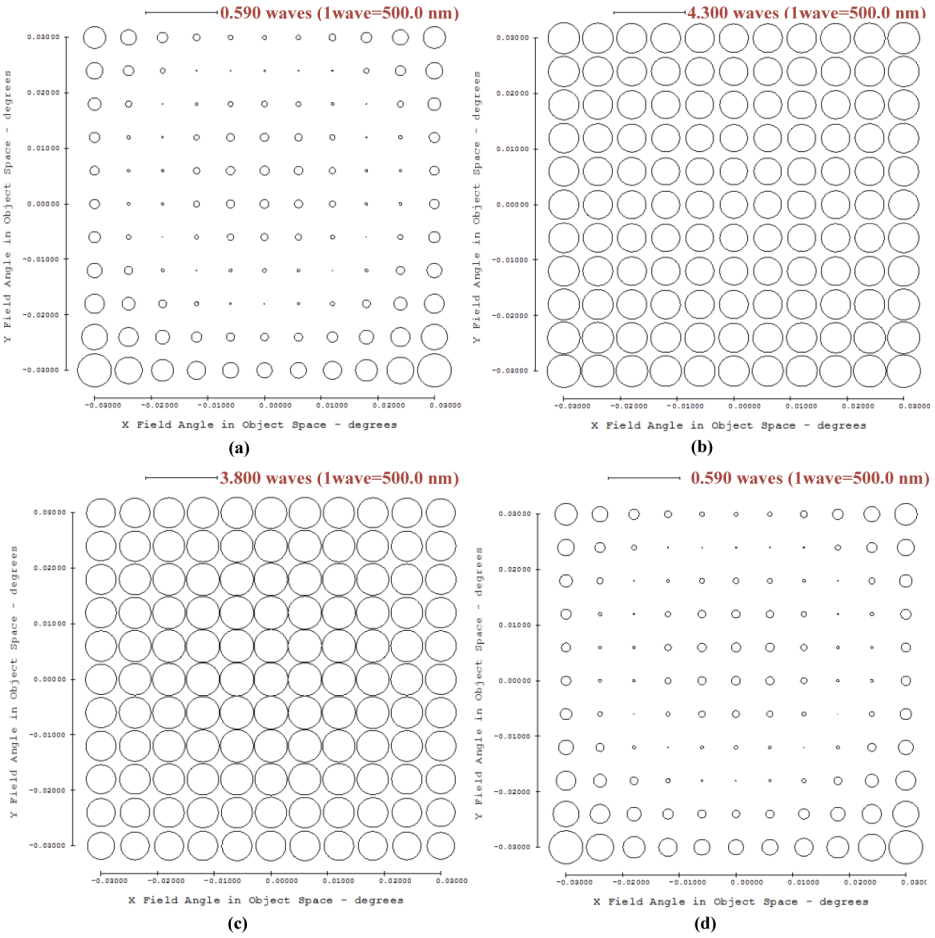

Fig. 4. FFDs for defocus aberration (Z4) in the NST in different cases. (a) shows defocus aberration in the nominal state, (b) shows the defocus aberration in ROC error of PM, (c) shows the defocus aberration in the presence of axis misalignments and (d) shows defocus aberration where the aberration (astigmatic and coma) induced by axial misalignments compensates the aberration (astigmatic and coma) induced by ROC error of the PM. (a) and (d) show that defocus aberration can be compensated as well in the process of compensation.

Optics EXPRESS

can be obtained as

$$\Delta W_{020r} = \frac{-2r_2^2[2(r_1+\Delta r_1)-2r_2-4d_1]^2D^2}{8[(r_1+\Delta r_1)r_2]^2(2r_1-2r_2-4d_1)^2}\Delta r_1 \approx \frac{-2D^2}{8r_1^2}\Delta r_1. \tag{19}$$

Referring to Eq. (16), the change of the distance between actual image plane and Gaussian image plane induced by axial misalignments can be derived as

$$\Delta l_{pF'} = \frac{4r_2^2}{(2r_1-2r_2-4d_1)^2}\Delta d_1. \tag{20}$$

Expressions for the relationship between ΔW_{020} and Δd_1 can be derived as

$$\Delta W_{020d_1} = \frac{4r_2^2[2(r_1+\Delta r_1)-2r_2-4d_1]^2D^2}{8[(r_1+\Delta r_1)r_2]^2(2r_1-2r_2-4d_1)^2}\Delta d_1 \approx \frac{4D^2}{8r_1^2}\Delta d_1. \tag{21}$$

Comparing Eq. (19) and Eq. (21), there is an interesting conclusion that ΔW_{020r} induced by ROC error and ΔW_{020d_1} induced by the axis misalignment satisfy the following relationship

$$\frac{\Delta W_{020r}}{\Delta W_{020d_1}} = -\frac{\Delta r_1}{2\Delta d_1}. \tag{22}$$

The conclusion that there is $\Delta W_{020} = 0$ when $\frac{\Delta r_1}{\Delta d_1} = 2$ exists is obtained from Eq. (22). Combining Eq. (12) with Eq. (22), ΔW_{020} is nearly zero after compensating the effects of ROC error using axial misalignments. In other words, the position of the focal image plane after aberration compensation is nearly the same as nominal state.

Here an example is used to demonstrate the statement presented above, as shown in Fig. 4. Here the specific ROC error of the PM is also $\Delta r_1 = -0.2$mm. It is shown that the net defocus aberration is nearly zero after compensation. In other words, astigmatism, coma and defocus aberration induced by ROC error can be compensated by axial misalignments together.

5. Other discussions

5.1. *Astigmatic and coma aberration field in pupil-offset off-axis two-mirror astronomical telescopes in the presence of the error of conic constant*

It is well known that the aberration induced by the error of conic constant is similar to the aberration induced by ROC error in on-axis two-mirror astronomical telescopes. Therefore, there are some similarities between the aberration induced by the error of conic constant and the ones induced by ROC error in pupil-offset off-axis two-mirror astronomical telescopes. In this section, it is discussed in detail how the aberration field can be affected by the error of conic constant for the most common case of the aperture stop located at the PM. The behavior of coma and astigmatism in the presence of the error of conic constant will be described.

The results of Eq. (3) show that the relationship between $W_{040}^{(sph,asph)}$ and the error of conic constant can be re-written as below

$$W_{040}^{(sph,asph)} = \sum_j W_{040oj}^{(sph,asph)} + K_{k_{PM}}\Delta k_{PM} + K_{k_{SM}}\Delta k_{SM}, \tag{23}$$

where

$$\begin{cases} K_{k_{PM}} = \frac{D^4m^3}{512(f'_{SYS})^3} \\ K_{k_{SM}} = \frac{D^4(1-m)^3\gamma}{512(f'_{SYS})^3} \end{cases}. \tag{24}$$

Optics EXPRESS

According to the Eq. (4) and Eq. (23), the net astigmatism and coma can be expressed as

$$\begin{cases} \Delta W_{ast} = 2(K_{k_{PM}}\Delta k_{PM} + K_{k_{SM}}\Delta k_{SM})\vec{s}^2 \\ \Delta W_{coma} = 4(K_{k_{PM}}\Delta k_{PM} + K_{k_{SM}}\Delta k_{SM})\vec{s} \end{cases}. \tag{25}$$

It is shown that a field-constant astigmatism and coma will be induced in the field of view in the presence of the error of conic constant. Besides, the directions of these two kinds of field constant aberration induced by the error of conic constant is related to the direction of pupil decenter.

Here we suppose the error of conic constant in the PM of NST is 0.0002 and the error of conic constant in the SM of NST also is 0.0002. The net astigmatism and coma are shown in Table 2, where column A represents the results obtained from optical simulation software for on-axis parent system, column B represent the results calculated with Eq. (25) for NST and column C represents the results obtained from optical simulation software for NST. Furthermore, the full field displays (FFDs) for astigmatism and coma over a ±0.03° field of view are shown in Fig. 5. Table 2 shows that the astigmatism and coma in NST is far more sensitive to ROC error than in its parent on-axis system (especially astigmatism). Figure 5 demonstrates that a field-constant astigmatism and coma are induced in the effective field of view, which is consistent with the Eq. (25).

Table 2. Verification for the Expressions Describing the Astigmatic Aberration Field and the Coma Aberration Field when there are $\Delta k_{PM} = 0.0002$ and $\Delta k_{SM} = 0.0002$ in NST and its Parent System

		A	B	C
$(0°, 0°)$	ΔC_5	0.00	−1.03	−0.86
	ΔC_6	0.00	0.00	0.00
	ΔC_7	0.00	0.00	0.00
	ΔC_8	0.00	0.30	0.23
$(0°, 0.03°)$	ΔC_5	0.00	−1.03	−0.85
	ΔC_6	0.00	0.00	0.00
	ΔC_7	0.00	0.00	0.00
	ΔC_8	0.00	0.30	0.23

5.2. Some discussions for segmented mirror telescopes

Segmented primary mirrors are efficient solutions to the problems with monolithic primary mirror manufacture, testing, transportation and launch. In fact, segmented mirror telescopes can be seen as an array of pupil-offset off-axis telescopes. In Section 4, it is shown that the effects of ROC error can well be compensated by axial misalignments. However, in this subsection, we will show that this is not the case for a segmented PM when different segments have a unique ROC error.

One special on-axis two-mirror optical system is designed, whose design parameters are consistent with NST (including ROC of each mirror and distance between PM and SM) except that PM is segmented and the entrance pupil diameter is 4252.85 mm. The size and position of each segment is similar to the PM of NST. The gap between different segment is 10 mm. Optical layout of this telescope and geometry of the segmented PM are presented in Fig. 6.

Here some random ROC errors are introduced to the PM segments, which are listed in Table 3. These ROC errors are randomly generated within the range of [0.01 mm, 0.02 mm], and the sign of these errors are also randomly selected. On the other hand, we can use the axial position of each PM segment to compensate for the effect of ROC error in each sub-aperture. The axial displacement of each segment used for compensating ROC error of itself is also listed in Table 3.

Optics EXPRESS

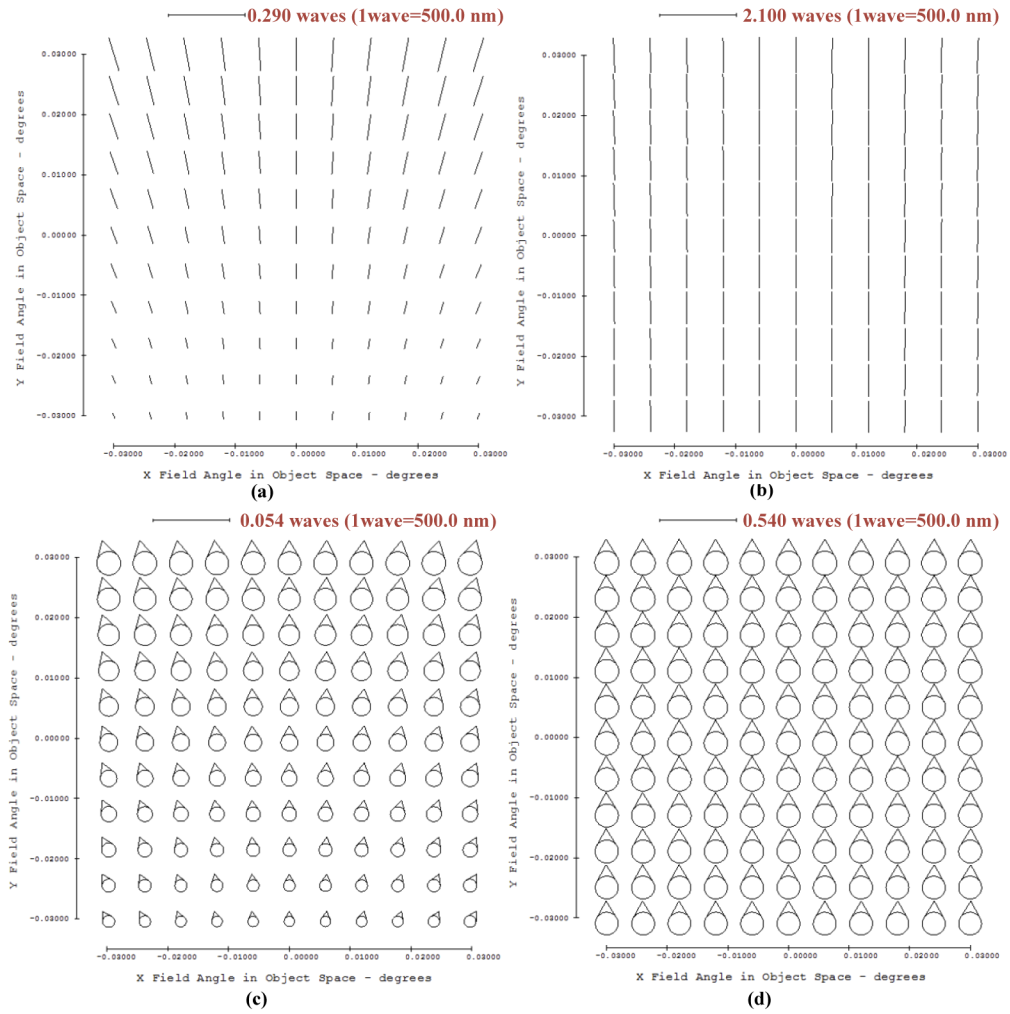

Fig. 5. FFDs for astigmatism (Z5/Z6) in the NST in nominal state (a) and in the presence of the error of conic constant (b). FFDs for coma (Z7/Z8) in the NST in nominal state (c) and in the presence of the error of conic constant (d). (b) and (d) show that in the presence of the error of conic constant, a large field-constant astigmatism and coma exists in the field of view.

Table 3. Introduced ROC error and the axial displacement of each segment used for compensating this error in each sub-aperture

Segment index	ROC Error/mm	Compensating Distance/mm
P1	0.017922	0.008961
P2	−0.019594	−0.009797
P3	0.016557	0.0082785
P4	−0.010357	−0.0051785
P5	−0.018491	−0.0092455
P6	0.019339	0.0096695

Optics EXPRESS

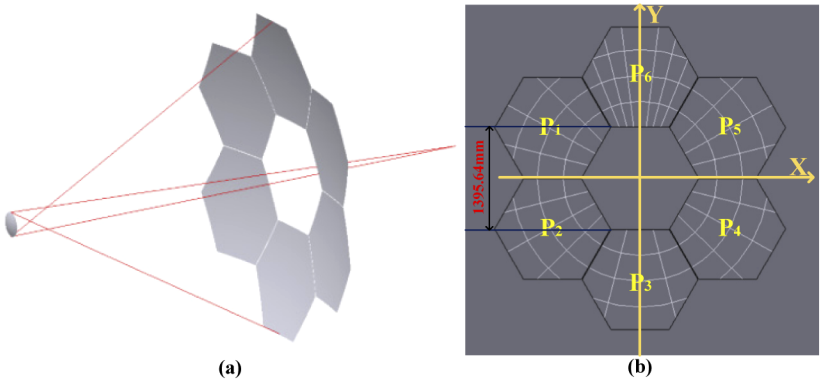

Fig. 6. Optical layout of the simulated on-axis two-mirror astronomical telescope with segmented PM obtained from CODE V (a) and geometry of the segmented PM with six segments (b).

The point spread functions (PSFs) at different wavelengths of this segmented system in nominal state are shown in Fig. 7(a) where the peak value of these PSFs is 100 times of the strehl ratio. The last PSF in Fig. 7(a) is a superposition of different wavelengths from 400 nm to 700 nm with a wavelength interval of 10 nm, which is used to simulate wide spectrum imaging. PSFs at different wavelengths of this segmented system with a unique ROC error in each segment are

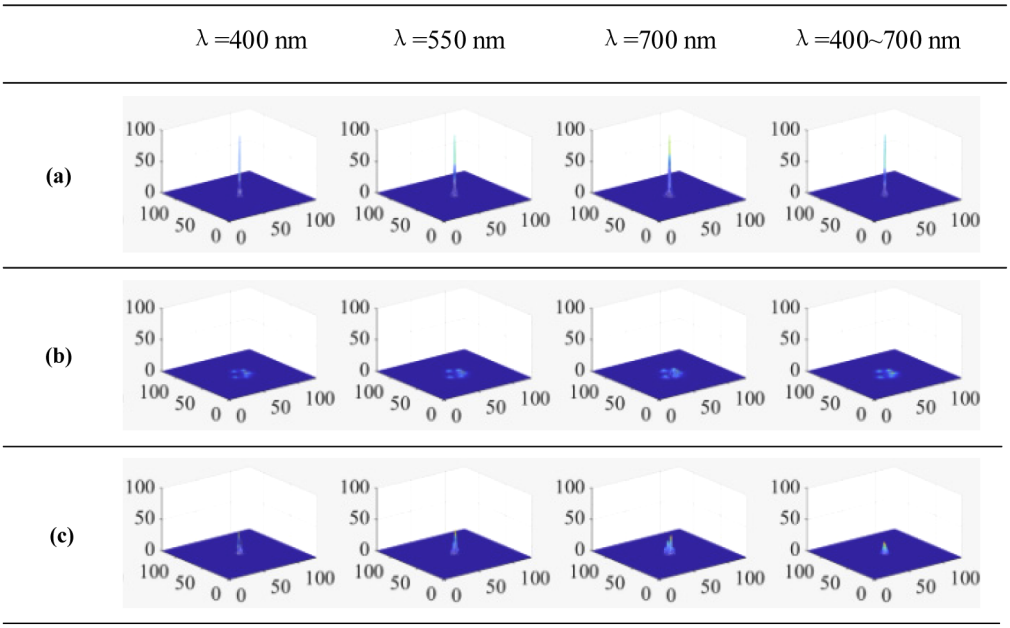

Fig. 7. (a) shows PSFs at different wavelengths and bandwidths in the nominal state. (b) shows PSFs at different wavelengths and bandwidths in the presence of ROC error of each segment. It is shown that in the presence of a unique ROC error in each PM segment, the strehl ratio of these PSFs are very low. (c) shows PSFs at different wavelengths and bandwidths when each PM segment is axially adjusted to compensate for the effect of ROC error for each sub-aperture. In this case, the figure of the PSF apparently change with wavelength and the strehl ratio decreases greatly for the case of wide spectrum imaging.

Optics EXPRESS

shown in Fig. 7(b). It is shown that in the presence of a unique ROC error in each PM segment, the strehl ratio of these PSFs at different wavelengths are very low compared to those in nominal state.

When each PM segment is axially adjusted to compensate for the effect of ROC error for each sub-aperture, the wavefront in sub-aperture is nearly corrected to the nominal state (each PM segment and SM compose an off-axis system and ROC error in PM segment can be compensated by introducing axial misalignment of PM segment, as discussed in the previous sections). However, in this case a phasing error is introduced between different sub-apertures. This phasing error not only can decrease the strehl ratio of the PSF at a single different wavelength, but also make the PSF change dramatically with wavelength. Therefore, in the case of wide spectrum imaging, the strehl ratio of the PSF will further be decreased. As shown in Fig. 7(c), the figure of the PSF apparently change with wavelength and the strehl ratio decreases greatly for the case of wide spectrum imaging.

Therefore, in the presence of a unique ROC error in each segment, the imaging quality will degrade, and this degrading effect cannot be compensated by introducing axial misalignments of each PM segment (the phasing error after compensation will also degrade the imaging quality, especially for wide spectrum imaging).

6. Conclusion

This paper systematically discusses the influences of ROC error in off-axis two-mirror astronomical telescopes, including the aberration field dependences, aberration compensation between ROC error and axial misalignments, the similarities between the effects of conic error and ROC error as well as the effect of ROC inconsistency in segmented telescopes. Some conclusions are presented below:

(1) A field-constant 0°astigmatism and 90°coma can be induced by ROC error in off-axis two-mirror telescopes (supposing the direction of pupil decenter lies in y direction).

(2) It is demonstrated that the net astigmatic and coma aberration field induced by ROC error can well be compensated by axial misalignments. Importantly, the focal plane shift induced by ROC error can also be compensated at the same time.

(3) The aberration field characteristics induced by conic error in off-axis two-mirror telescopes is very similar with those induced by ROC error.

(4) In segmented telescopes, the effects of ROC inconsistency cannot not be compensated by axially adjusting each PM segments. While the aberrations in each sub-aperture can well be compensated, a phasing error will be introduced between different sub-apertures, which will degrade the imaging quality, especially for wide spectrum imaging.

The first conclusion and third conclusion presented above are not only applicable to off-axis two-mirror telescopes, but also applicable to off-axis optical telescopes with more mirrors, except that some small field-dependent aberration terms will be introduced when the system have a larger field. The last conclusion is applicable to general segmented telescopes.

Besides, the effects of ROC error can also be compensated by axial misalignments, which is applicable to general optical systems. However, only when the axial position of the PM is used to compensate for the ROC error of the PM (the position and ROC of the other mirrors stay unchanged), the focal plane will stay unchanged.

Appendix A: Optical prescription and layout of the NST telescope

The optical prescription of the NST is presented in Table 4 and the layout of the NST is shown in Fig. 8.

Optics EXPRESS

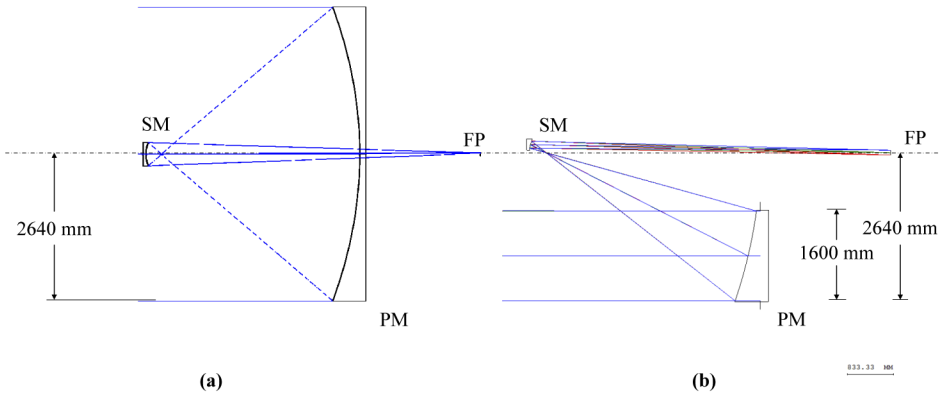

Fig. 8. (a) Layout of on-axis parent system of the NST telescope with fold mirrors removed. (b) Layout of the NST telescope with fold mirrors removed. NST can be seen as an off-axis portion of the parent on-axis telescope.

Table 4. Optical Prescription of the NST Telescope with Fold Mirrors Removed

	Radius/mm	Conic	Thickness/mm
PM	−7700	−1	−4150.05
SM	573.5828	−0.83087	6490.259
FP	FLAT	0.00000	

Appendix B

In this Appendix, we will provide the derivation process of Eq. (12). Considering that the conic of the PM is Equal to −1 (or very close to −1), the expression of spherical aberration shown in Eq. (3) can be simplified as

$$W_{040}^{(sph,asph)} = \frac{D^4(m+1)^2(1-m)\gamma}{512(f'_{SYS})^3} + \frac{k_{SM}D^4(1-m)^3\gamma}{512(f'_{SYS})^3}, \tag{26}$$

Note that $m \equiv -\frac{f'_{SYS}}{f'_{PM}} = -\frac{d_2}{f'_1-d_1}$, $\gamma = \frac{y_{SM}}{y_{PM}} = 1 - \frac{2d_1}{r_1}$, and $f'_{SYS} = \frac{r_1 r_2}{2r_1-2r_2-4d_1}$ are all functions of r_1 and d_1 [18]. Here we first derive the sensitivity of $W_{040}^{(sph,asph)}$ to r_1:

$$\frac{\partial W_{040}^{(sph,asph)}}{\partial r_1} = A_1 + B_1 + C_1 + A_2 + B_2 + C_2, \tag{27}$$

where

$$\begin{cases} A_1 = (1-2m-3m^2)\frac{2d_2}{(2d_1-r_1)^2}\gamma\frac{D^4}{512(f'_{SYS})^3} \\ B_1 = (1+m-m^2-m^3)\frac{2d_1}{r_1^2}\frac{D^4}{512(f'_{SYS})^3} \\ C_1 = (1+m-m^2-m^3)\gamma\frac{-3D^4}{512(f'_{SYS})^4}\frac{(-2r_2^2-4r_2d_1)}{(2r_1-2r_2-4d_1)^2} \\ A_2 = k_{SM}(-3+6m-3m^2)\frac{2d_2}{(2d_1-r_1)^2}\gamma\frac{D^4}{512(f'_{SYS})^3} \\ B_2 = k_{SM}(1-3m+3m^2-m^3)\frac{2d_1}{r_1^2}\frac{D^4}{512(f'_{SYS})^3} \\ C_2 = k_{SM}(1-3m+3m^2-m^3)\gamma\frac{-3D^4}{512(f'_{SYS})^4}\frac{(-2r_2^2-4r_2d_1)}{(2r_1-2r_2-4d_1)^2} \end{cases}. \tag{28}$$

Optics EXPRESS

Equation (28) can be further rewritten as

$$\frac{\partial W_{040}^{(sph,asph)}}{\partial r_1} = A_1 + E_1 + A_2 + E_2, \tag{29}$$

where

$$\begin{aligned} E_1 &= B_1 + C_1 \\ &= (1 + m - m^2 - m^3)\frac{D^4}{512(f'_{SYS})^3}\left[\frac{2d_1}{r_1^2} - \frac{3\gamma}{f'_{SYS}}\frac{(-2r_2^2 - 4r_2d_1)}{(2r_1 - 2r_2 - 4d_1)^2}\right] \\ &= (1 + m - m^2 - m^3)\frac{D^4}{512(f'_{SYS})^3}\left[\frac{3r_1r_2 + 8r_1d_1 - 8r_2d_1 - 16d_1^2}{r_1^2(r_1 - r_2 - 2d_1)}\right], \end{aligned} \tag{30}$$

$$\begin{aligned} E_2 &= B_2 + C_2 \\ &= k_{SM}(1 - 3m + 3m^2 - m^3)\frac{D^4}{512(f'_{SYS})^3}\left[\frac{2d_1}{r_1^2} + \frac{-3\gamma}{f'_{SYS}}\frac{(-2r_2^2 - 4r_2d_1)}{(2r_1 - 2r_2 - 4d_1)^2}\right] \\ &= k_{SM}(1 - 3m + 3m^2 - m^3)\frac{D^4}{512(f'_{SYS})^3}\left[\frac{3r_1r_2 + 8r_1d_1 - 8r_2d_1 - 16d_1^2}{r_1^2(r_1 - r_2 - 2d_1)}\right]. \end{aligned} \tag{31}$$

The sensitivity of $W_{040}^{(sph,asph)}$ to d_1 can be expressed as

$$\frac{\partial W_{040}^{(sph,asph)}}{\partial d_1} = I_1 + J_1 + K_1 + I_2 + J_2 + K_2, \tag{32}$$

where

$$\begin{cases} I_1 = (1 - 2m - 3m^2)\frac{-4d_2}{(2d_1 - r_1)^2}\gamma\frac{D^4}{512(f'_{SYS})^3} \\ J_1 = (1 + m - m^2 - m^3)\frac{-2}{r_1}\frac{D^4}{512(f'_{SYS})^3} \\ K_1 = (1 + m - m^2 - m^3)\gamma\frac{-3D^4}{512(f'_{SYS})^4}\frac{4r_1r_2}{(2r_1 - 2r_2 - 4d_1)^2} \\ I_2 = k_{SM}(-3 + 6m - 3m^2)\frac{-4d_2}{(2d_1 - r_1)^2}\gamma\frac{D^4}{512(f'_{SYS})^3} \\ J_2 = k_{SM}(1 - 3m + 3m^2 - m^3)\frac{-2}{r_1}\frac{D^4}{512(f'_{SYS})^3} \\ K_2 = k_{SM}(1 - 3m + 3m^2 - m^3)\gamma\frac{-3D^4}{512(f'_{SYS})^4}\frac{4r_1r_2}{(2r_1 - 2r_2 - 4d_1)^2} \end{cases}, \tag{33}$$

Equation (33) can further be rewritten as

$$\frac{\partial W_{040}^{(sph,asph)}}{\partial d_1} = I_1 + L_1 + I_2 + L_2, \tag{34}$$

where

$$\begin{aligned} L_1 &= J_1 + K_1 \\ &= (1 + m - m^2 - m^3)\frac{D^4}{512(f'_{SYS})^3}\left[\frac{-2}{r_1} + \frac{-3\gamma}{f'_{SYS}}\frac{4r_1r_2}{(2r_1 - 2r_2 - 4d_1)^2}\right] \\ &= (1 + m - m^2 - m^3)\frac{D^4}{512(f'_{SYS})^3}\left[\frac{-8r_1^2 + 2r_1r_2 + 16r_1d_1}{r_1^2(r_1 - r_2 - 2d_1)}\right], \end{aligned} \tag{35}$$

Optics EXPRESS

$$\begin{aligned} L_2 &= J_2 + K_2 \\ &= k_{SM}(1-3m+3m^2-m^3)\frac{D^4}{512(f'_{SYS})^3}\left[\frac{-2}{r_1}+\frac{-3\gamma}{f'_{SYS}}\frac{4r_1r_2}{(2r_1-2r_2-4d_1)^2}\right] \\ &= k_{SM}(1-3m+3m^2-m^3)\frac{D^4}{512(f'_{SYS})^3}\left[\frac{-8r_1^2+2r_1r_2+16r_1d_1}{r_1^2(r_1-r_2-2d_1)}\right]. \end{aligned} \tag{36}$$

On one hand, we can recognize that

$$\frac{A_1}{I_1} = \frac{A_2}{I_2} = -\frac{1}{2}. \tag{37}$$

On the other hand, we can further obtain that

$$\begin{aligned} \frac{E_1}{L_1} = \frac{E_2}{L_2} &= \frac{\frac{3r_1r_2+8r_1d_1-8r_2d_1-16d_1^2}{r_1^2(r_1-r_2-2d_1)}}{\frac{-8r_1^2+2r_1r_2+16r_1d_1}{r_1^2(r_1-r_2-2d_1)}} \\ &= \frac{3r_1r_2+8r_1d_1-8r_2d_1-16d_1^2}{-8r_1^2+2r_1r_2+16r_1d_1} \\ &= \frac{3r_1r_2+4d_1(2r_1-2r_2-4d_1)}{-2r_1(4r_1-r_2-8d_1)} \\ &= \frac{3+\frac{4d_1}{f'_{SYS}}}{-2\left(4\frac{r_1}{r_2}-1-8\frac{d_1}{r_2}\right)}. \end{aligned} \tag{38}$$

For two-mirror astronomical telescopes, we can have the following equations from the principle of optical design [18]:

$$\begin{cases} r_1 = \frac{2(-d_1)f'_{SYS}}{d_2-f'_{SYS}} \\ r_2 = \frac{2(-d_1)d_2}{d_2-d_1-f'_{SYS}} \end{cases}. \tag{39}$$

By substitute Eq. (39) into Eq. (38), we can obtain

$$\begin{aligned} \frac{E_1}{L_1} = \frac{E_2}{L_2} &= \frac{3+\frac{4d_1}{f'_{SYS}}}{-2\left[4\frac{f'_{SYS}(d_2-d_1-f'_{SYS})}{d_2(d_2-f'_{SYS})}-1+\frac{4(d_2-d_1-f'_{SYS})}{d_2}\right]} \\ &= -\frac{1}{2}\left[\frac{(3f'_{SYS}+4d_1)(d_2-f'_{SYS})}{4f'_{SYS}(d_2-d_1-f'_{SYS})-(d_2-f'_{SYS})f'_{SYS}}\right] \\ &= -\frac{1}{2}\left[1+\frac{4d_1d_2}{3d_2f'_{SYS}-4d_1f'_{SYS}-3(f'_{SYS})^2}\right]. \end{aligned} \tag{40}$$

In general, for astronomical telescopes, the focal length of the system, f'_{SYS}, is far larger than d_1 and d_2. For example, $|f'_{SYS}|$ of NST is about 80000 mm, while $|d_1|$ and $|d_2|$ are about 4000 mm and 6500 mm, respectively. Therefore, we can also obtain

$$\frac{E_1}{L_1} = \frac{E_2}{L_2} = -\frac{1}{2}. \tag{41}$$

By combining Eq. (37) and Eq. (41), we can finally have

$$\frac{K_{040r_1}}{K_{040d_1}} = \frac{\frac{\partial W_{040}^{(sph,asph)}}{\partial r_1}}{\frac{\partial W_{040}^{(sph,asph)}}{\partial d_1}} = \frac{A_1+A_2+E_1+E_2}{I_1+I_2+L_1+L_2} = -\frac{1}{2}. \tag{42}$$

Optics EXPRESS

Funding

National Key Research and Development Program of China (2016YFE0205000); National Natural Science Foundation of China (61705223, 61905241, 62805235).

Disclosures

The authors declare that there are no conflicts of interest related to this article.

References

1. R. J. R. Kuhn and S. L. Hawley, "Some astronomical performance advantages of off-axis telescopes," Publ. Astron. Soc. Pac. **111**(759), 601–620 (1999).
2. F. Zeng, X. Zhang, J. Zhang, G. Shi, and H. Wu, "Optics ellipticity performance of an unobscured off-axis space telescope," Opt. Express **22**(21), 25277–25285 (2014).
3. R. V. Shack and K. P. Thompson, "Influence of alignment errors of a telescope system," Proc. SPIE **0251**, 146–153 (1980).
4. K. P. Thompson, "Aberration fields in tilted and decentered optical systems," Ph.D. dissertation (University of Arizona, Tucson, Arizona, 1980).
5. K. Thompson, "Description of the 3rd-order optical aberrations of near-circular pupil optical systems without symmetry," J. Opt. Soc. Am. A **22**(7), 1389–1401 (2005).
6. K. P. Thompson, "Multinodal 5th-order optical aberrations of optical systems without rotational symmetry: spherical aberration," J. Opt. Soc. Am. A **26**(5), 1090–1100 (2009).
7. K. P. Thompson, "Multinodal 5th-order optical aberrations of optical systems without rotational symmetry: the comatic aberrations," J. Opt. Soc. Am. A **27**(6), 1490–1504 (2010).
8. K. P. Thompson, "Multinodal 5th-order optical aberrations of optical systems without rotational symmetry: the astigmatic aberrations," J. Opt. Soc. Am. A **28**(5), 821–836 (2011).
9. T. Schmid, K. P. Thompson, and J. P. Rolland, "Misalignment-induced nodal aberration fields in two-mirror astronomical telescopes," Appl. Opt. **49**(16), D131–D144 (2010).
10. K. P. Thompson, T. Schmid, and J. P. Rolland, "The misalignment induced aberrations of TMA telescopes," Opt. Express **16**(25), 20345–20353 (2008).
11. G. Ju, C. Yan, Z. Gu, and H. Ma, "Aberration fields of off-axis two-mirror astronomical telescopes induced by lateral misalignments," Opt. Express **24**(21), 24665–24703 (2016).
12. G. Ju, C. Yan, Z. Gu, and H. Ma, "Nonrotationally symmetric aberrations of off-axis two-mirror astronomical telescopes induced by axial misalignments," Appl. Opt. **57**(6), 1399–1409 (2018).
13. G. Ju, H. Ma, and C. Yan, "Aberration fields of off-axis astronomical telescopes induced by rotational misalignments," Opt. Express **26**(19), 24816–24834 (2018).
14. A. Cornejo and D. Malacara, "Required accuracy in the radius of curvature of a primary astronomical telescope mirror," Boletin Del Instituto De Tonantzintla 1 (1975).
15. J. Rakoczy, D. Hall, W. Ly, R. Howard, and E. Montgomery, "Global Radius of Curvature Estimation and Control for the Hobby-Eberly Telescope," Proc. SPIE **4837**, 681–692 (2003).
16. D. Cheng, Y. Wang, M. M. Talha, J. Chang, and H. Hua, "Effect of radius mismatch on performance of segmented telescopic systems," Proc. SPIE **6834**, 68341Y (2007).
17. J. Wang, B. Guo, Q. Sun, and Z. Lu, "Third-order aberration fields of pupil decentered optical systems," Opt. Express **20**(11), 11652–11658 (2012).
18. R. N. Wilson, *Reflecting Telescope Optics*, 2nd ed. (SpringerVerlag, 2004), Vols. 3 and 4.
19. X. Bai, G. Ju, H. Ma, and S. Xu, "Aberrational interactions between axial and lateral misalignments in pupil-offset off-axis two-mirror astronomical telescopes," Appl. Opt. **58**(28), 7693–7707 (2019).